Experimental, Observational, and Theoretical Constraints on the Nuclear Symmetry Energy

J. M. Lattimer

Department of Physics & Astronomy

STONY BROOK UNIVERSITY

U.S. DEPARTMENT OF ENERGY
Office of Science

Astrophysical neutrinos and the origin of the elements
INT, Seattle, Washington, July 31, 2023

Acknowledgements

Funding Support:

DOE - Nuclear Physics

DOE - Toward Exascale Astrophysics of Mergers and Supernovae (TEAMS)

NASA - Neutron Star Interior Composition ExploreR (NICER)

NSF - Neutrinos, Nuclear Astrophysics and Symmetries (PFC - N3AS)

DOE - Nuclear Physics from Multi-Messenger Mergers (NP3M)

Recent Collaborators:

Duncan Brown & Soumi De (Syracuse), Christian Drischler, Madappa Prakash & Tianqi Zhao (Ohio), Sophia Han (TDLI), Evgeni Kolomeitsev (Matej Bei, Slovakia), Akira Ohnishi (YITP, Kyoto), Sanjay Reddy (INT), Achim Schwenk (Darmstadt), Andrew Steiner (Tennessee) & Ingo Tews (LANL)

Nuclear Symmetry Energy and Pressure

The symmetry energy is the difference between the energies of pure neutron matter ($x=0$) and symmetric ($x=1/2$) nuclear matter:

$$S(n)=E(n,x=0)-E(n,x=1/2).$$

The quadratic term in an expansion of neutron excess $1-2x$ dominates:
$E(n,x)=E(n,1/2)+(1-2x)^2S_2(n)+$
Expanding S_2 about saturation n_s:

$$S_2(n)=\mathbf{J}+\frac{\mathbf{L}}{3}\frac{n-n_s}{n_s}+\ldots$$

$$\mathbf{J}\simeq 31\ \mathrm{MeV},\quad \mathbf{L}\simeq 50\ \mathrm{MeV}$$

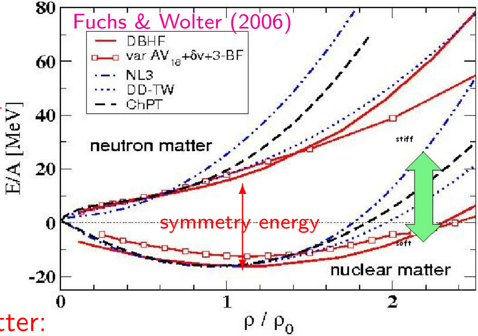

Extrapolated to pure neutron matter:
$E_N=E(n_s,0)\approx J+E(n_s,1/2)\equiv J-B,\qquad P_N=P(n_s,0)=Ln_s/3$
Neutron star matter (beta equilibrium) is nearly neutron matter:

$$\frac{\partial(E+E_e)}{\partial x}=0,\quad P_{NSM}(n_s)\simeq\frac{Ln_s}{3}\left[1-\left(\frac{4J}{\hbar c}\right)^3\frac{4-3J/L}{3\pi^2n_s}\right]$$

Why is the Symmetry Energy Important?

The equation of state in a neutron star depends strongly on the density dependance of the symmetry energy ($u = n_B/n_s$):

$$P_{NSM}(u) \simeq n_s u^2 \left[\frac{L}{3} + \frac{K_N}{9}(u-1) + \frac{Q_N}{54}(u-1)^2 + \cdots\right].$$

A strong correlation exists between radii and P_{NSM} near n_s: $R_{1.4} \sim P_{NSM}(n_B)^{1/4}$.

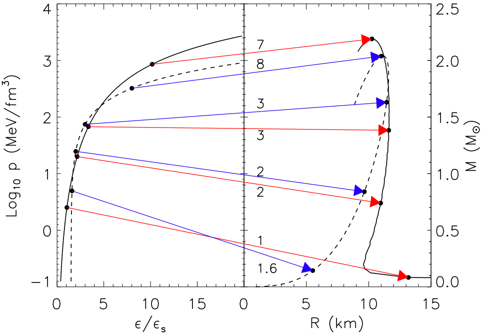

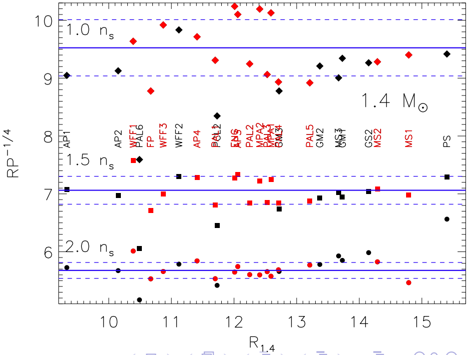

Fitting Nuclear Binding Energies

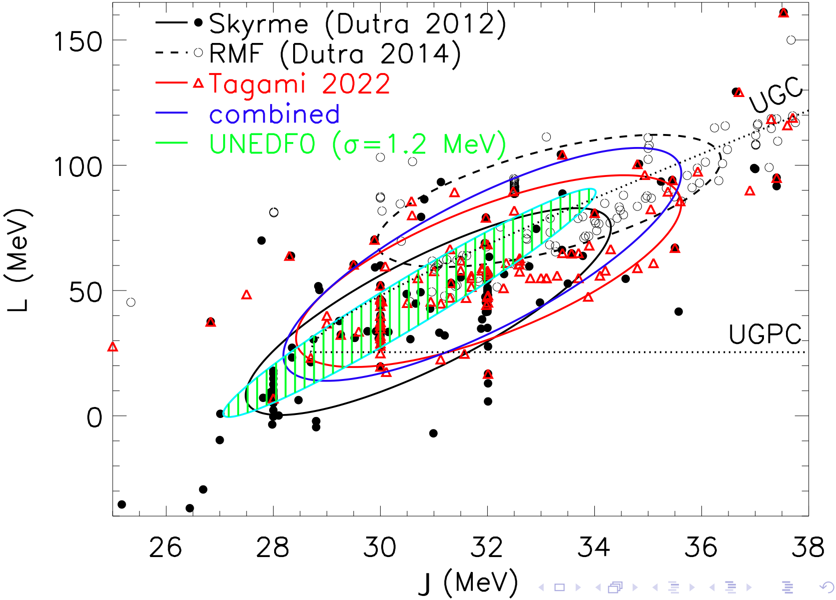

Meaning of $J - L$ Correlations

The slope dL/dJ is an indicator of the most sensitive density u_s for the measurement of the symmetry energy $S(u)$.

If the correlation line goes through (J, L), a change dJ can be compensated by a change dL.

$$\frac{dJ}{dL} = -\left(\frac{\partial S(u_s)}{\partial L}\right)_J \Bigg/ \left(\frac{\partial S(u_s)}{\partial J}\right)_L .$$

Example: $S(u) = S_K u^{2/3} + S_V u^\gamma, \quad S_K \simeq 12.5 \text{ MeV}$
$J = S_K + S_V, \quad L = 2S_K + 3\gamma S_V = S_K(2 - 3\gamma) + 3\gamma J$

$$\frac{dJ}{dL} = -\frac{\ln u_s}{3}, \quad u_s = \exp\left(-3\frac{dJ}{dL}\right).$$

For binding energies, $dL/dJ \simeq 11, \quad u_s \simeq 0.76$.

Saturation Properties of Nuclear Interactions

Empirical Saturation Window

$B = 16.06 \pm 0.20$ MeV

$n_s = 0.1558 \pm 0.0054$ fm^{-3}

$K_{1/2} = 236.5 \pm 15.4$ MeV

Data from Dutra (2012, 2014)

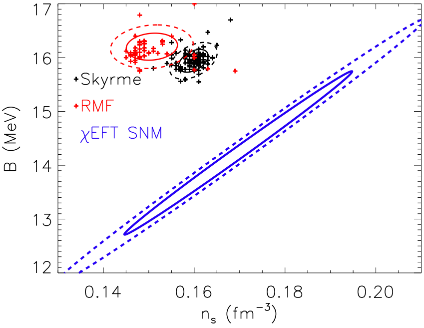

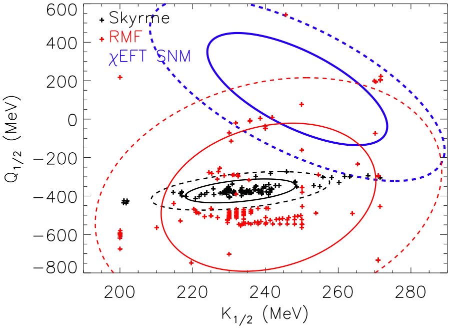

Theoretical Neutron Matter Studies

Recently developed chiral effective field theory allows a systematic expansion of nuclear forces at low energies based on the symmetries of quantum chromodynamics. It exploits the gap between the pion mass (the pseudo-Goldstone boson of chiral symmetry-breaking) and the energy scale of short-range nuclear interactions established from experimental phase shifts. It provides the only known consistent framework for estimating energy uncertainties.

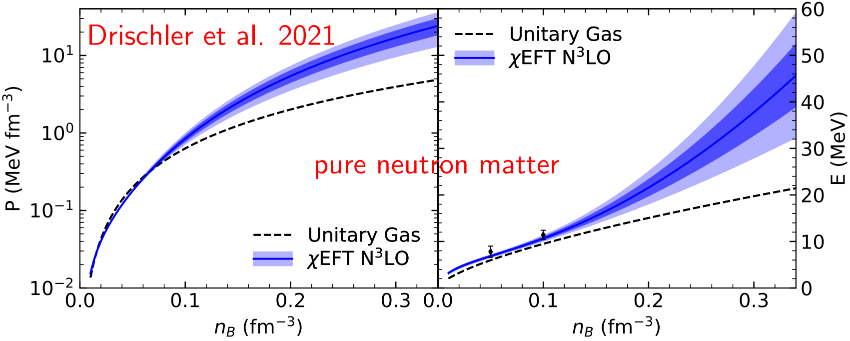

Symmetry Parameters From Chiral EFT

Two approaches to extracting J and L

symmetric matter

1. Take the difference between pure neutron and symmetric matter energies and pressures at the calculated saturation density.

2. Use pure neutron matter energy and pressure with the empirical saturation window from nuclear mass fits.

$J = E_N(n_s) + B,$

$L = 3P_N(n_s)/n_s.$

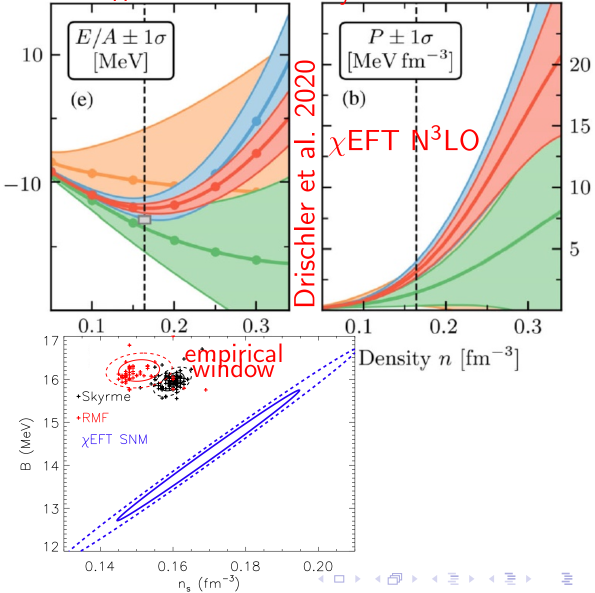

Symmetry Parameters From Neutron Matter

Pure neutron matter calculations are more reliable than symmetric matter calculations.

Symmetric matter emerges from a delicate cancellation sensitive to short- and intermediate-range three-body interactions at N^2LO that are Pauli-blocked in pure neutron matter.

N^3LO symmetric matter calculations don't saturate within empirical ranges for n_s and B, and introduce spurious correlations in symmetric matter.

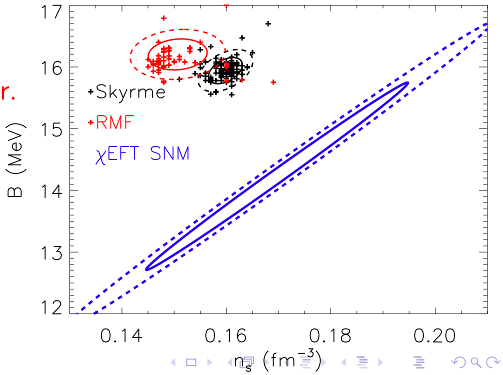

We infer symmetry parameters from $E_N(n_s)$ and $P_N(n_s)$ using

$$J = E_N(n_s) + B$$

$$L = 3P_N(n_s)/n_s$$

and include uncertainties in E_N, P_N, n_s and B.

Correlations From Chiral EFT

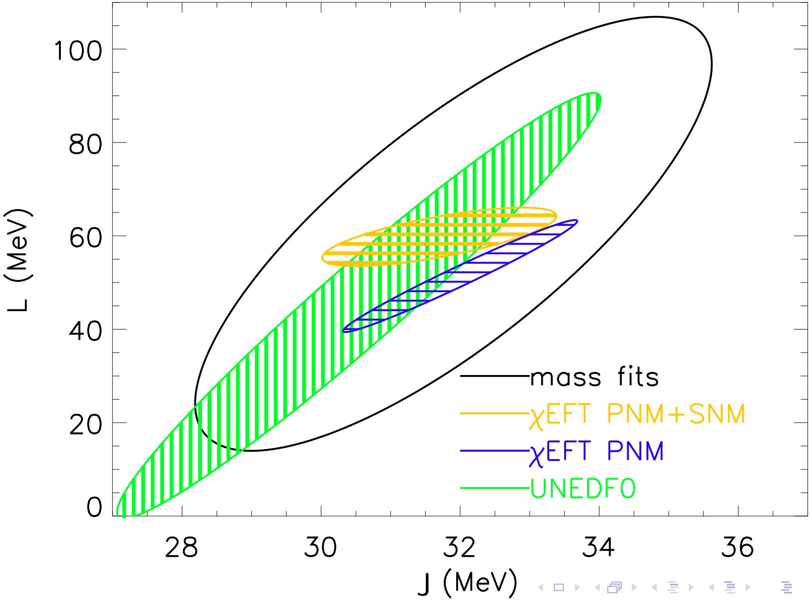

Bounds From The Unitary Gas Conjecture

The Conjecture (UGC):
Neutron matter energy always larger than unitary gas energy.
$E_{UG} = \xi_0 (3/5) E_F$, or

$$E_{UG} \simeq 12.6 \left(\frac{n}{n_s}\right)^{2/3} \mathrm{MeV}.$$

The unitary gas consists of fermions interacting via a pairwise short-range s-wave interaction with infinite scattering length and zero range. Cold atom experiments show a universal behavior with the Bertsch parameter $\xi_0 \simeq 0.37$.

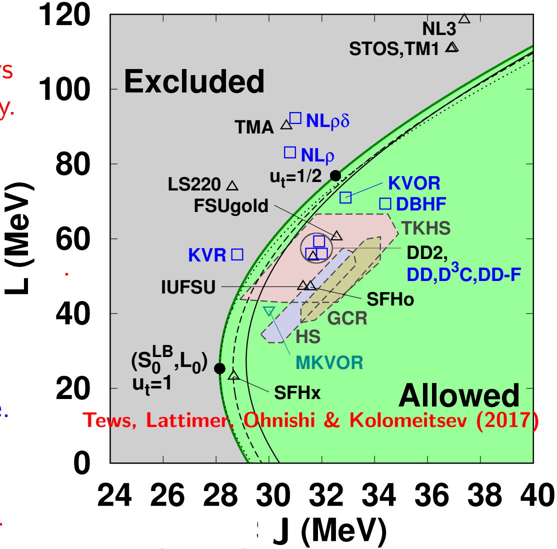

For $n \geq n_s$, one also observes $P_N > P_{UG}$ (UGPC).
$J \geq 28.6$ MeV; $L \geq 25.3$ MeV; $P_N(n_s) \geq 1.35$ MeV fm^{-3}; $R_{1.4} \geq 9.7$ km

Applying Unitary Gas Constraints

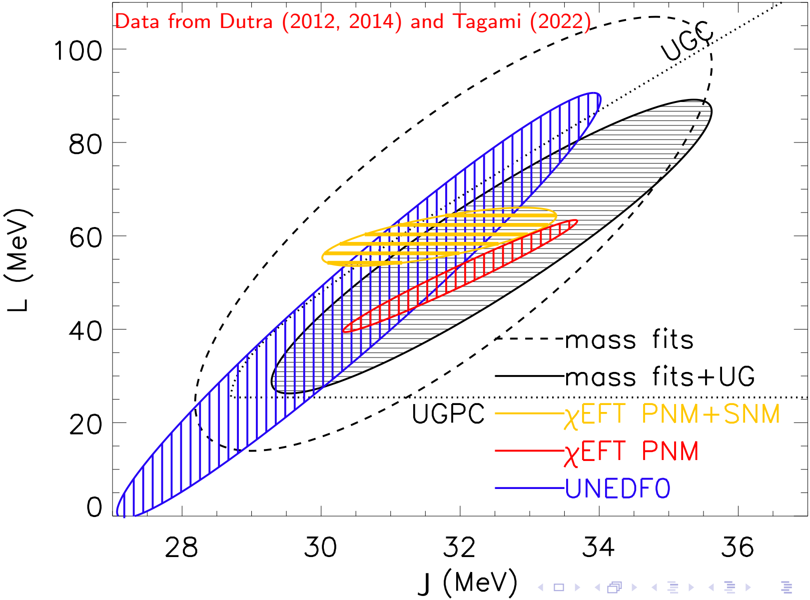

Neutron Skin Thickness

The difference between the mean neutron and proton radii in the liquid droplet model is

$t_{np} = R_n - R_p$.

The mean square difference is

$r_{np}^2 =< R_n >^2 - < R_p >^2$.

$$r_{np} = \sqrt{\frac{3}{5}}\frac{2r_oI}{3}\frac{S_s}{J}\left[1 + S_sA^{-1/3}/J\right]^{-1} f_C$$

Implies strong $L - r_{np}$ correlation.

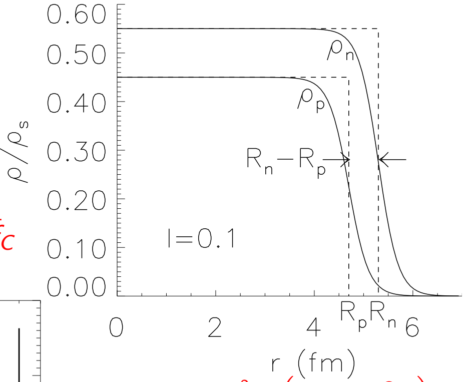

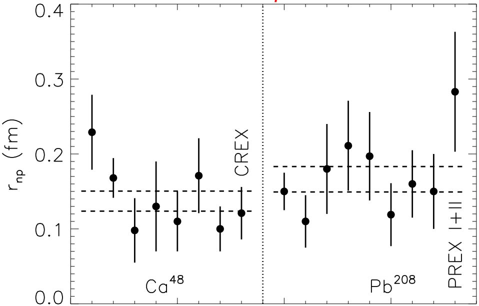

$$f_C = 1 - \frac{3Ze^2}{140IS_Sr_o}\left(1 + \frac{10S_S}{3JA^{1/3}}\right)$$

For ^{208}Pb: $r_{np} \simeq 0.13$ fm

$$\frac{\Delta(S_S/J)}{\Delta J} \simeq -0.020$$

$$\frac{\Delta L}{\Delta J} = \frac{\Delta(S_S/J)}{\Delta J}\frac{1}{0.0234} \simeq -0.84$$

Calculated $L - r_{np}$ Correlations

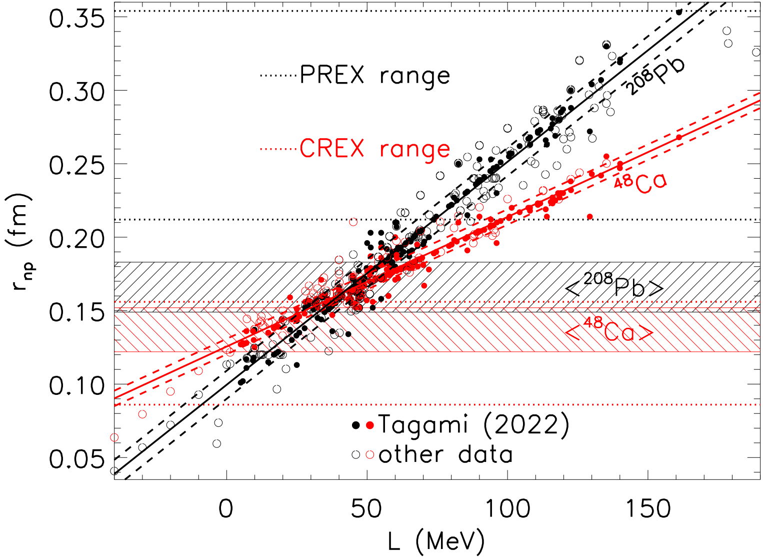

Implied L Values

Historical experimental weighted average ^{208}Pb
$r_{np}^{208} = 0.166 \pm 0.017$ fm, implying $L = 45 \pm 13$ MeV.

Historical experimental weighted average ^{48}Ca
$r_{np}^{48} = 0.137 \pm 0.015$ fm, implying $L = 14 \pm 21$ MeV.

Combined $L = 36 \pm 11$ MeV.

Parity-violating electron scattering measurements at JLab:

PREX I+II ^{208}Pb (Adhikari et al. 2021):
$r_{np}^{208} = 0.283 \pm 0.071$ fm, implying $L = 119 \pm 46$ MeV.

CREX ^{48}Ca (Adhikari et al. 2022):
$r_{np}^{48} = 0.121 \pm 0.035$ fm, implying $L = -5 \pm 42$ MeV.

Combined $L = 51 \pm 31$ MeV.

$r_{np}^{208} - r_{np}^{48}$ Linear Correlation

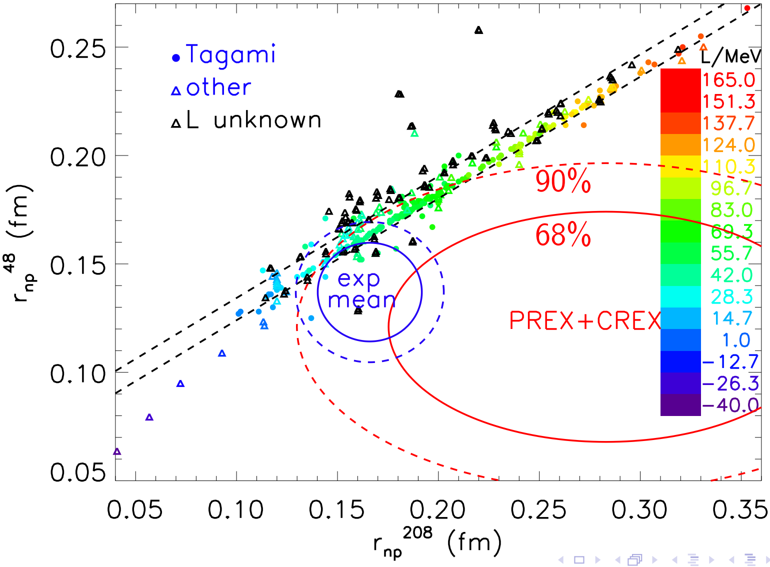

Detail

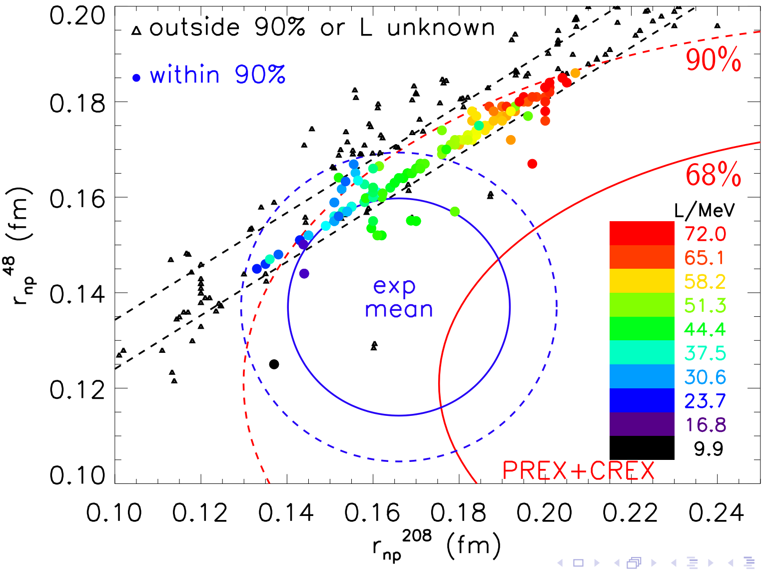

outside 90% or L unknown
within 90%
90%
68%
exp mean
PREX+CREX
L/MeV
72.0
65.1
58.2
51.3
44.4
37.5
30.6
23.7
16.8
9.9
0.20
0.18
0.16
0.14
0.12
0.10
r_{np}^{48} (fm)
0.10 0.12 0.14 0.16 0.18 0.20 0.22 0.24
r_{np}^{208} (fm)

Implied $J - L$

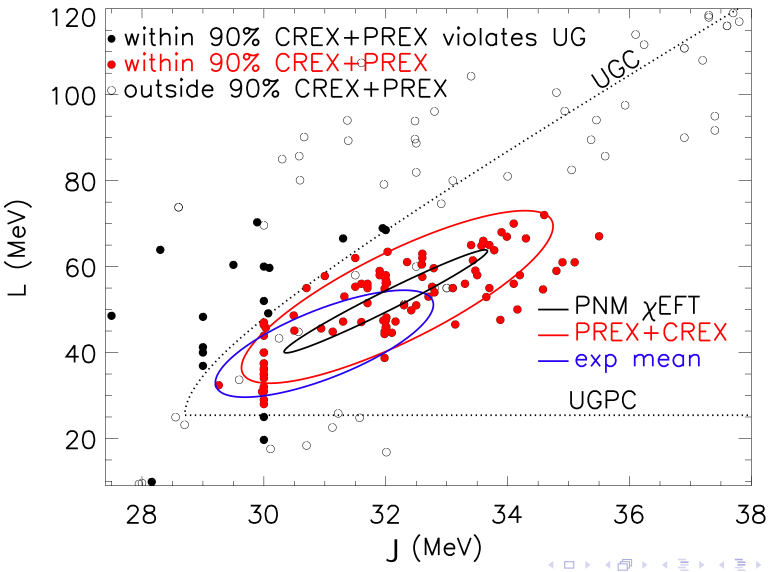

120
100
80
60
40
20
28
30
32
34
36
38
J (MeV)
L (MeV)
within 90% CREX+PREX violates UG
within 90% CREX+PREX
outside 90% CREX+PREX
UGC
PNM χEFT
PREX+CREX
exp mean
UGPC

The Radius – Pressure Correlation

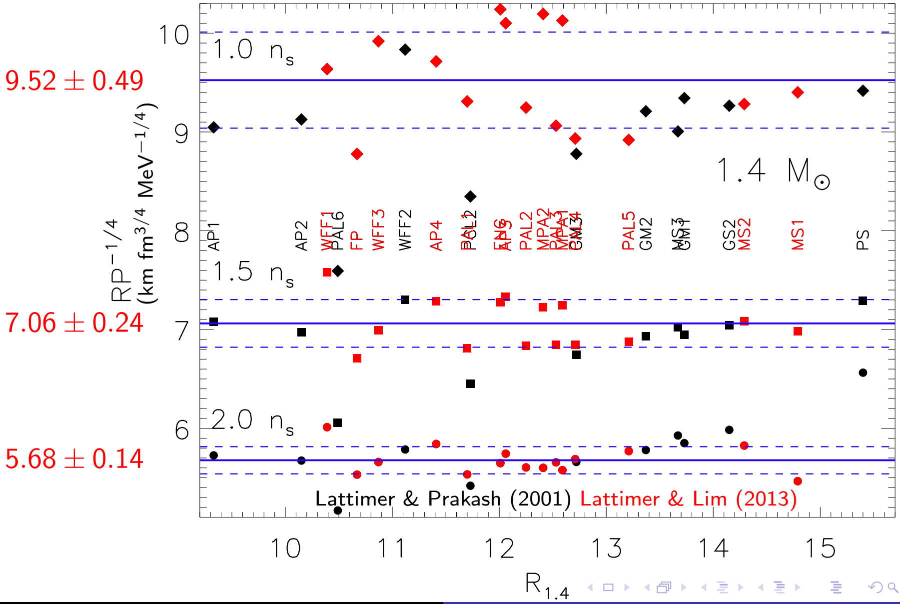

Implied $R_{1.4} - L$

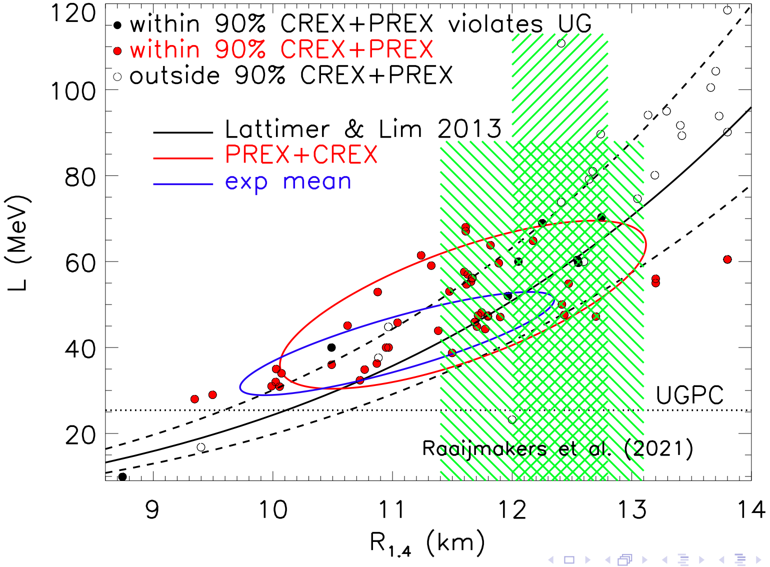

Neutron Star Interior Composition ExploreR (NICER)

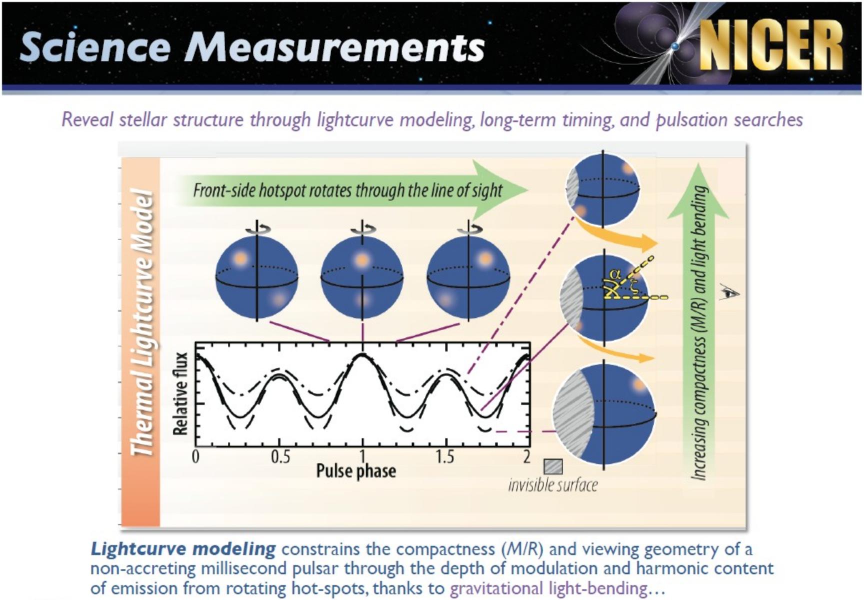

Science Measurements (cont.) NICER

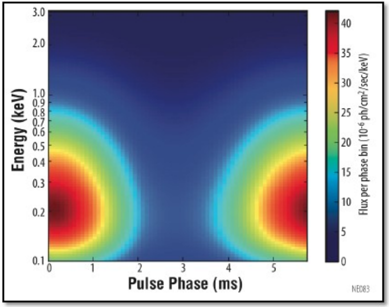

… while phase-resolved spectroscopy promises a direct constraint of radius *R*.

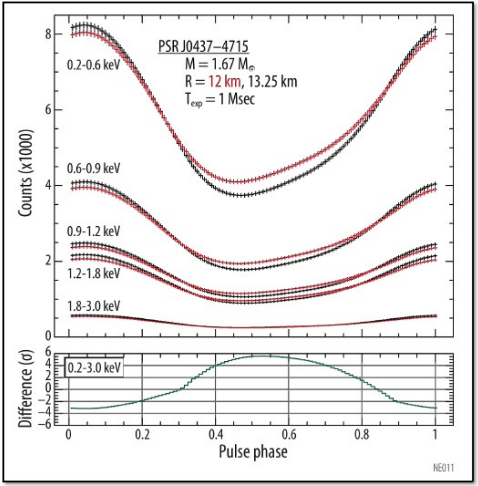

GW170817

- LVC detected a signal consistent with a BNS merger, followed 1.7 s later by a weak gamma-ray burst.
- $\simeq$ 10100 orbits observed over 317 s.
- $\mathcal{M} = 1.186 \pm 0.001\ M_\odot$
- $M_{\rm T,min} = 2^{6/5}\mathcal{M} = 2.725 M_\odot$
- $E_{\rm GW} > 0.025 M_\odot c^2$
- $D_L = 40^{+8}_{-14}$ Mpc
- $75 < \tilde{\Lambda} < 560$ (90%)
- $M_{\rm ejecta} \sim 0.06 \pm 0.02\ M_\odot$
- Blue ejected mass: $\sim 0.01 M_\odot$
- Red ejected mass: $\sim 0.05 M_\odot$
- Probable r-process production
- Ejecta + GRB: $M_{max} \lesssim 2.22 M_\odot$

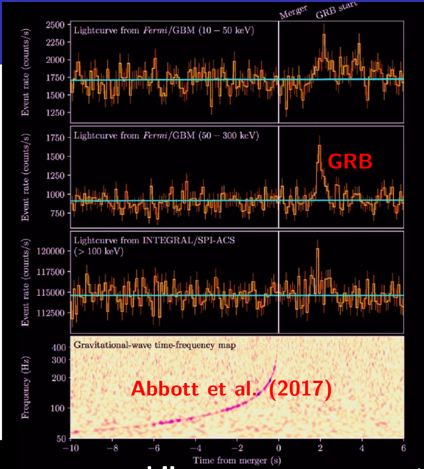

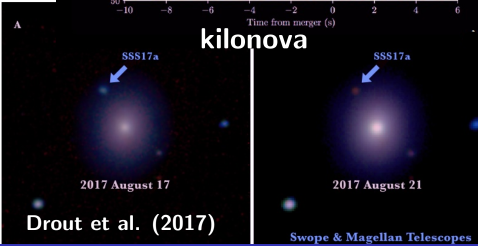

Binary Deformability and the Radius

$$\tilde{\Lambda} = \frac{16}{13}\frac{(1+12q)\Lambda_1 + q^4(12+q)\Lambda_2}{(1+q)^5} \simeq \frac{16a}{13}\left(\frac{R_{1.4}c^2}{G\mathcal{M}}\right)^6 \frac{q^{8/5}(12-11q+12q^2)}{(1+q)^{26/5}}.$$

This is very insensitive to q for $q > 0.5$, so

$$\tilde{\Lambda} \simeq a' \left(\frac{R_{1.4}c}{G\mathcal{M}}\right)^6 .$$

For $\mathcal{M} = (1.2 \pm 0.2)\ M_\odot$, $a' = 0.0035 \pm 0.0006$,

$$R_{1.4} = (11.5 \pm 0.3)\frac{\mathcal{M}}{M_\odot}\left(\frac{\tilde{\Lambda}}{800}\right)^{1/6} \mathrm{km}.$$

For GW170817, $\mathcal{M} = 1.186 M_\odot$, $a' = 0.00375 \pm 0.00025$,

$$R_{1.4} = (13.4 \pm 0.1)\left(\frac{\tilde{\Lambda}}{800}\right)^{1/6} \mathrm{km}.$$

Implied $\Lambda_{1.4} - L$

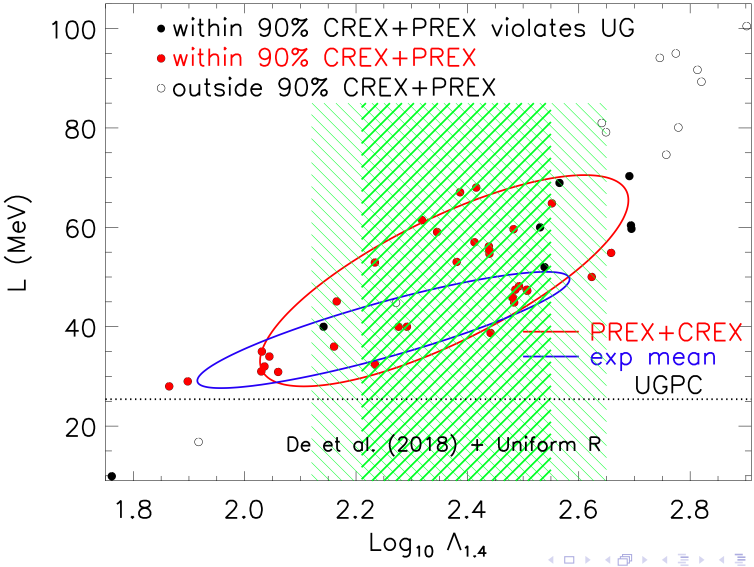

Summary of Astrophysical Observations

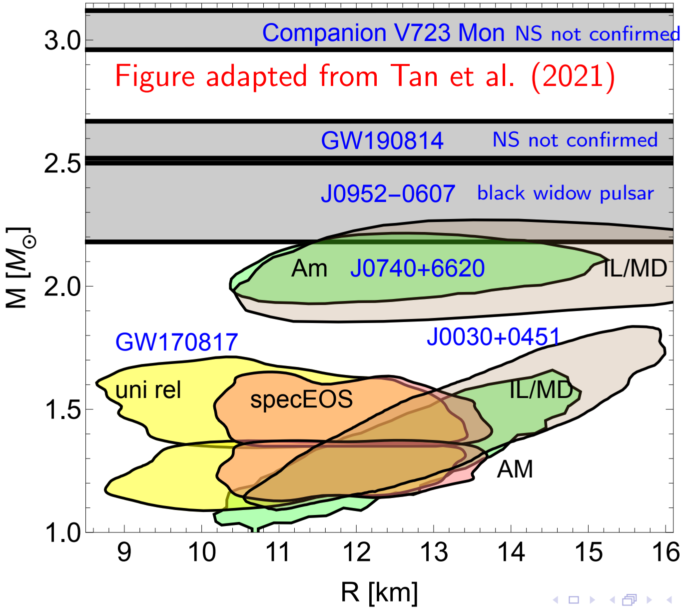

Moment of Inertia

- Spin-orbit coupling is of same magnitude as post-post-Newtonian effects (Barker & O'Connell 1975, Damour & Schaeffer 1988).
- Precession alters orbital inclination angle (observable if system is face-on) and periastron advance (observable if system is edge-on).
- More EOS sensitive than R: $I \propto MR^2$.
- Measurement requires system to be extremely relativistic.
- Double pulsar PSR J0737-3037 is an edge-on candidate; $M_A = 1.338185^{+12}_{-14} M_\odot$.
- Even more relativistic systems are likely to be found, based on faintness and nearness of PSR J0737-3037.

Recent Moment of Inertia Measurement

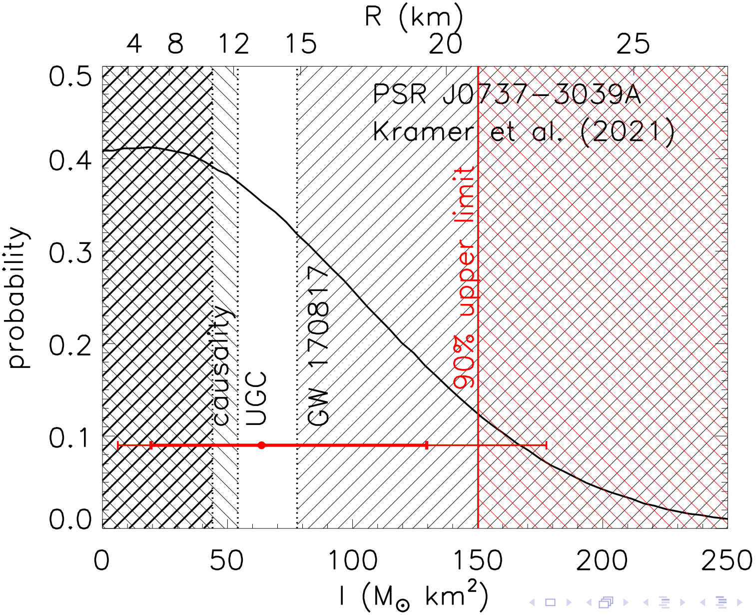

S190426c: First Black Hole-Neutron Star Merger?

Information from LVC indicated a marginal case, with 58% chance of being 'terrestrial anomaly'.

Assuming it is cosmic in origin, GCN circular 24411 stated $p_{\rm BHNS} = 0.60, p_{\rm gap} = 0.35, p_{\rm BNS} = 0.15, p_{\rm BBH} < 0.01$, $p_{\rm HasNS} > 0.99$ and $p_{\rm rem} = 0.72$.

LVC defined BNS if both $M_{1,2} \le 3M_\odot$, BH if both $M_{1,2} \ge 5M_\odot$ and gap if either mass satisfied $3M_\odot < M < 5M_\odot$.

LVC won't immediately release the chirp mass $\mathcal{M}$ (even though it's known precisely), the mass ratio $q = M_1/M_2 > 1$ (and therefore M_1 and M_2, known much less precisely), and the spin parameter χ if one component is a BH.

But it is still possible to recover $\mathcal{M}, M_1, M_2$ and χ in cases where $p_{\rm BHNS}, p_{\rm gap}, p_{BNS}$ and/or $p_{\rm rem}$ are nonzero.

Suitable Variables

$\mathcal{M}$ has small uncertainty $\sigma_{\mathcal{M}}$.

q has large uncertainty, but $q \in [1, \infty]$.

$\bar{q} = \ln(q-1)$ has $\bar{q} \in [-\infty, \infty]$ and large uncertainty σ_q.

σ_q is the most important parameter.

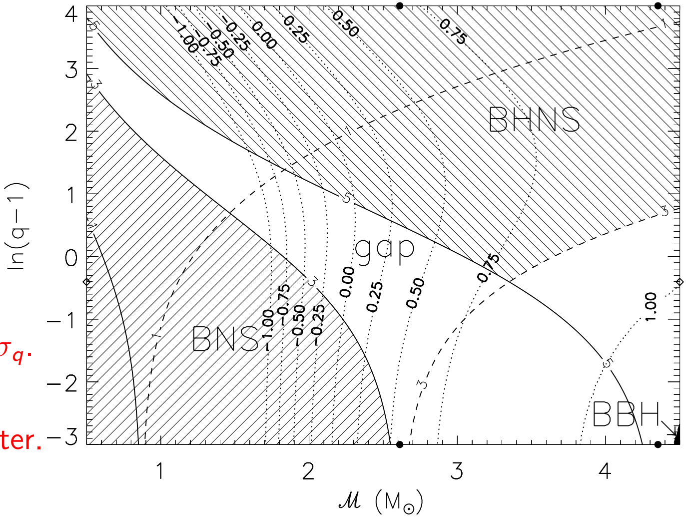

Probabilities

Assume

$$\frac{d^2p}{d\mathcal{M}d\bar{q}} = \frac{1}{2\pi\sigma_{\mathcal{M}}\sigma_q}\exp\left[-\frac{(\mathcal{M}-\mathcal{M}_0)^2}{2\sigma_{\mathcal{M}}^2} - \frac{(\bar{q}-\bar{q}_0)^2}{2\sigma_q^2}\right].$$

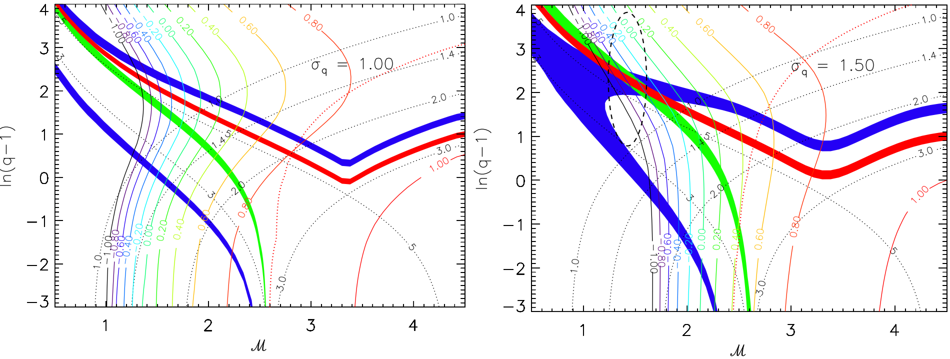

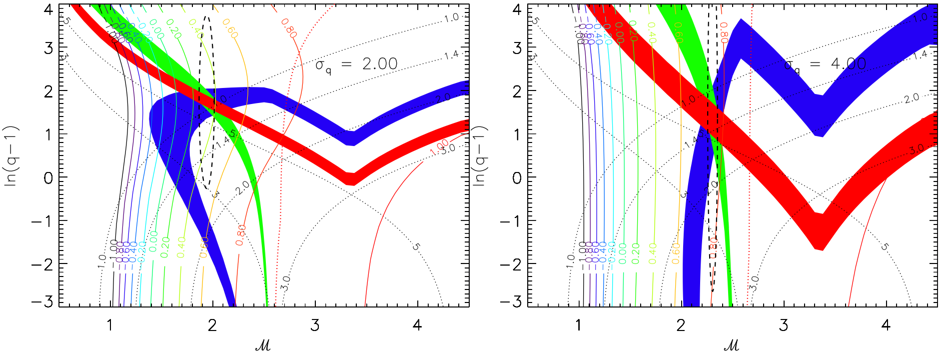
σq = 2.00
σq = 4.00
ln(q−1)
M

Spin

LVC uses model of Foucart et al. (2012, 2018) to determine mass M_d remaining outside the remnant more than a few ms after a BHNS merger:

$$M_d/M^b_{\rm NS} \simeq \alpha'\eta^{-1/3}(1-2\beta) - \hat{R}_{\rm ISCO}\beta\beta'\eta^{-1} + \gamma',$$

$\beta = GM_{\rm NS}/R_{\rm NS}c^2$, $\eta = q(1+q)^{-2}$ and
$\hat{R}_{\rm ISCO} = R_{\rm ISCO}c^2/GM_{\rm BH}$. $\alpha' \simeq 0.406$, $\beta' \simeq 0.139$, $\gamma' = 0.255$.

For the Kerr metric

$$\chi = \sqrt{\hat{R}_{\rm ISCO}}\left(4/3 - \sqrt{\hat{R}_{\rm ISCO}/3 - 2/9}\right).$$

$M_d = 0$ implies

$$\hat{R}_{\rm ISCO} = (\beta'\beta)^{-1}(\alpha'\eta^{2/3}(1-2\beta) + \gamma'\eta).$$

χ is found from $p_d = \int\int_{M_d \geq 0} \frac{d^2p}{d\mathcal{M}d\bar{q}} d\mathcal{M}d\bar{q}$.

Convergence For Large σ_q

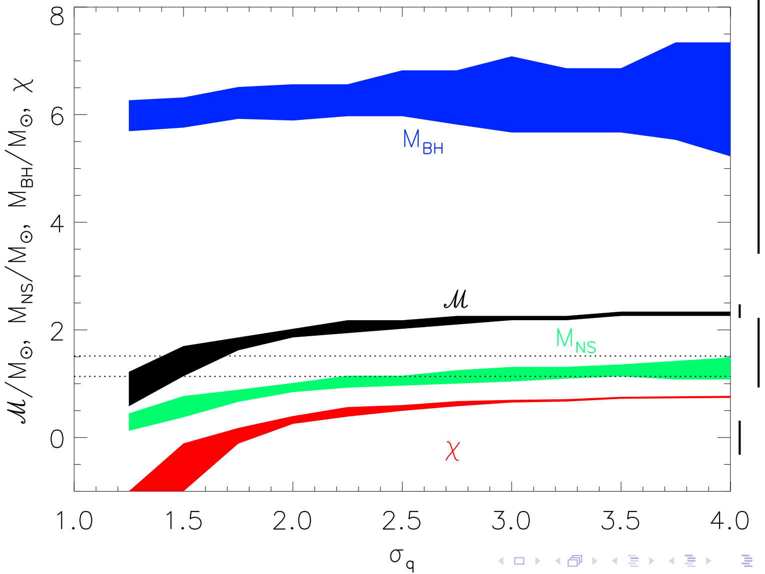

New LIGO/VIRGO/KAGRA Detections 2023

HasGap: probability that one object is between $3M_\odot$ and $5M_\odot$.

HasNS: probability that one object is between $1M_\odot$ and M_{max}.

rem: probability of disc formation.

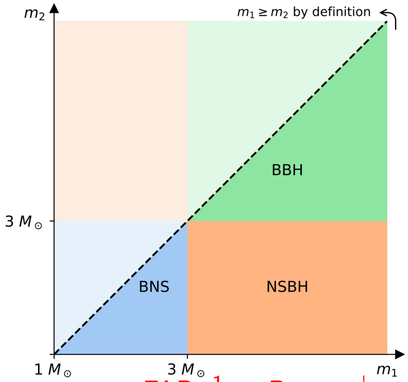

source	$p_{\rm BNS}$	$p_{\rm BHNS}$	$p_{\rm BBH}$	$p_{\rm Gap}$	$p_{\rm NS}$	$p_{\rm rem}$	$\rm FAR_{yr}^{-1}$	$D_{\rm Mpc}$
230518h	0.0	0.96	0.04	0.0	1.0	0.0	98	204 ± 57
230528a	0.31	0.69	0.0	0.97	1.0	0.02	9.6	261 ± 108
230529ay	0.33	0.67	0.0	0.98	1.0	0.12	160	201 ± 63
230615az	1.0	0.0	0.0	0.00	1.0	1.0	4.7	124 ± 34
230627c	0.0	0.51	0.49	0.26	0.0	0.0	100	278 ± 68

S230518h

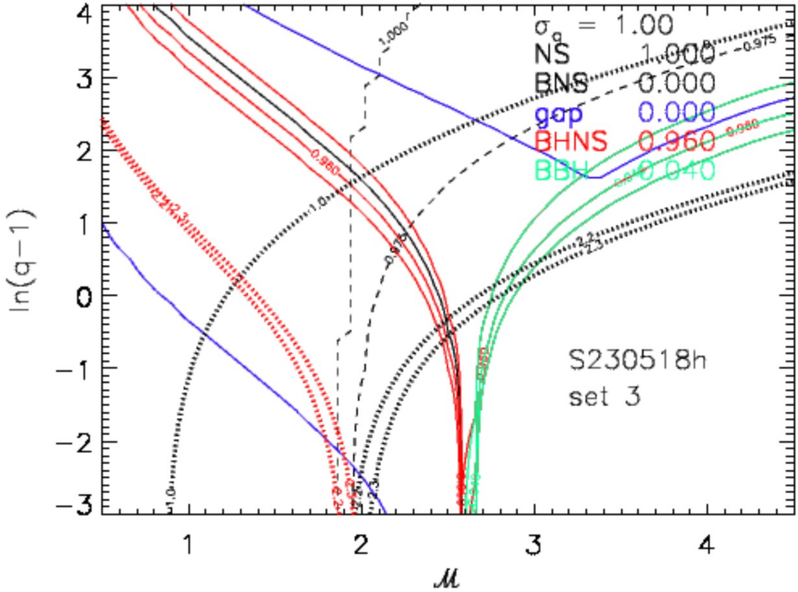

σ_q = 1.00
NS 1.000
BNS 0.000
gap 0.000
BHNS 0.960
BBH 0.040
S230518h
set 3
ln(q−1)
$\mathcal{M}$

S230529ay

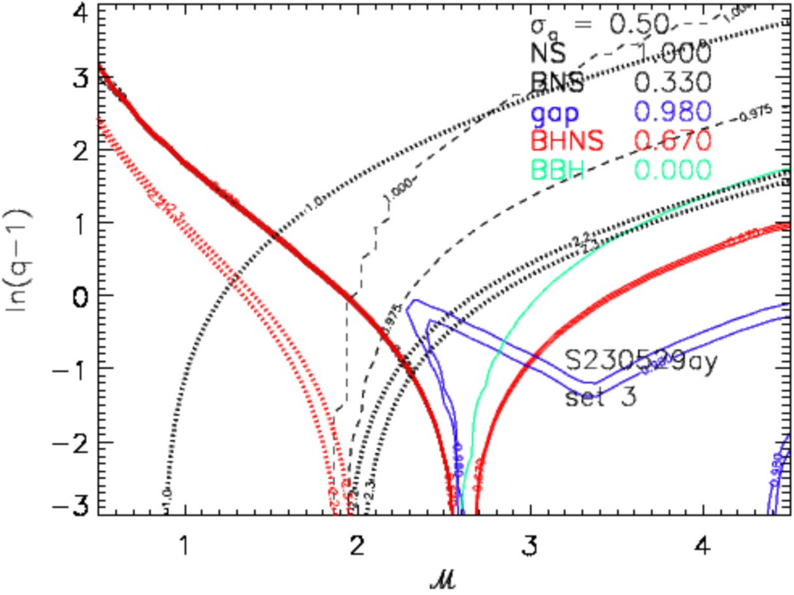

σ_q = 0.50
NS 1.000
BNS 0.330
gap 0.980
BHNS 0.670
BBH 0.000
S230529ay
set 3
ln(q−1)
$\mathcal{M}$

S230529ay

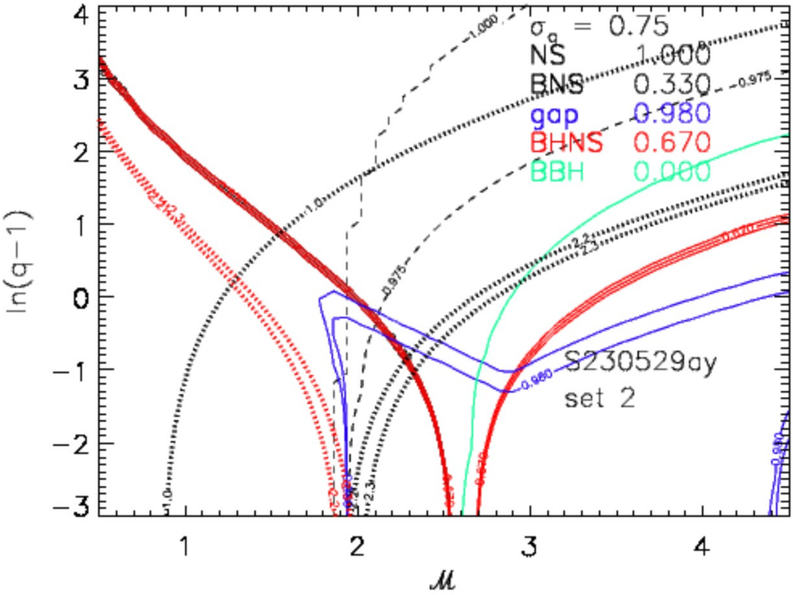

σ_q = 0.75
NS 1.000
BNS 0.330
gap 0.980
BHNS 0.670
BBH 0.000
S230529ay
set 2
ln(q−1)
$\mathcal{M}$

S230627c

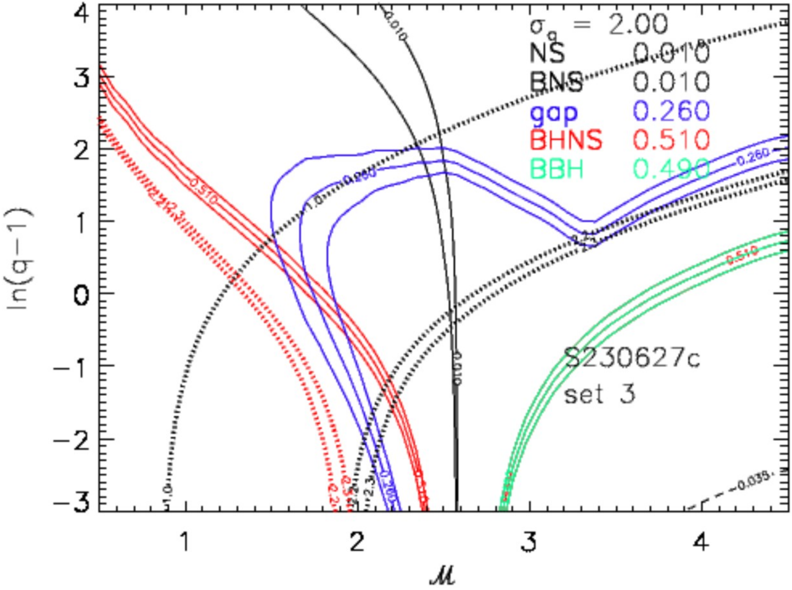

σq = 2.00
NS 0.010
BNS 0.010
gap 0.260
BHNS 0.510
BBH 0.490
S230627c
set 3
ln(q−1)
M

S230627c

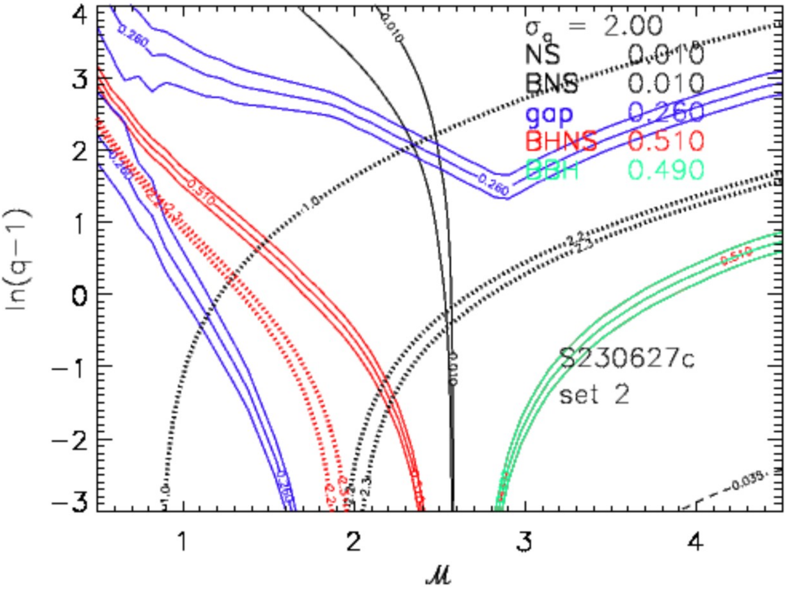

σ_q = 2.00
NS 0.010
BNS 0.010
gap 0.260
BHNS 0.510
BBH 0.490
S230627c
set 2
ln(q−1)
$\mathcal{M}$

Conclusions

Nuclear experiments and theory, including EDF fits to nuclear binding energies, chiral EFT calculations, and neutron skin and dipole polarizability measurements of ^{48}Ca and ^{208}Pb, consistently predict narrow ranges for the symmetry energy parameters **without any astrophysical inputs**:

$$J = (32\pm2)\ \mathrm{MeV}, \quad L = (50\pm10)\ \mathrm{MeV}, \quad K_N = (140\pm70)\ \mathrm{MeV}.$$

Neutron star radius predictions are about $R_{1.4} = (11.5 \pm 1.0)$ km.

This is consistent with inferences from GW170817, NICER X-ray timing measurements and X-ray observations of quiescent thermal and photospheric radius expansion burst sources.

We eagerly anticipate new neutron skin and dipole polarizability experiments, LIGO/Virgo/Kagra observations of neutron star mergers, radio pulsar timing measurements of masses and moments of inertia measurements, and NICER and other planned X-ray telescope observations of neutron stars.